Proceedings of International Conference on Heat Exchanger Fouling and Cleaning - 2015 (Peer-reviewed)
June 07 - 12, 2015, Enfield (Dublin), Ireland
Editors: M.R. Malayeri, H. Müller-Steinhagen and A.P. Watkinson

Published online
www.heatexchanger-fouling.com

REVIEW AND A CONCEPTUAL MODEL OF EXHAUST GAS RECIRCULATION (EGR) COOLER FOULING DEPOSITION AND REMOVAL MECHANISM

T. Han[1*], A.C. Booth[2], S. Song[2], D.J. Styles[3] and J.W. Hoard[1*]

[1] Department of Mechanical Engineering, University of Michigan, Ann Arbor, MI 48109, United States.
*E-mail: taehoonh@umich.edu, hoardjw@umich.edu
[2] Department of Automotive Engineering, University of Michigan, Ann Arbor, MI 48109, United States.
[3] Ford Motor Company, RIC Building, P.O. Box 2053, Dearborn, MI 48121, United States.

ABSTRACT

Exhaust gas recirculation (EGR) is essential to reduce NOx in engines, and EGR coolers are generally used to reduce the recirculated gas temperature. A common problem with the EGR cooler is a reduction of the effectiveness due to deposit layer. Typically, effectiveness rapidly decreases at first and then asymptotically stabilizes over time. The general outline of these phenomena is demonstrated here from the literature.

Various experiments on this stabilization have been reported. There are several hypotheses of the stabilizing phenomena; one of the possible theories is a deposit removal mechanism. When the removal mechanism has the feature that the removal rate equals to the deposit mass rate, then stabilization of the effectiveness occurs. In contrast, some reported experiments contradict this hypothesis. So, this paper attempts to compare and review the mechanism up to this time. Additionally, based on these studies, a conceptual model is suggested and compared to existing data.

INTRODUCTION

Exhaust Gas Recirculation (EGR) is used in diesel and gasoline vehicles to reduce NOx (Oxides of Nitrogen) for complying with emission regulations. As years go by the regulations are being strengthened for environmental protection all over the world. Consequently the usage of EGR is expected to be far higher.

Recirculating a portion of exhaust gas to the engine lowers the flame temperature and NOx due to reduced peak in-cylinder temperature. As part of the EGR system, EGR coolers are used to reduce the recirculated gas temperature. A main problem with the EGR cooler is, however, a reduction of the effectiveness due to the inside fouling layer caused by deposition of exhaust gas components such as soot, organic compounds, and water and acid. Also, this fouling phenomenon causes NOx emission increase, higher pressure drop, and fuel efficiency loss. Typically, the effectiveness rapidly decreases at first and then asymptotically stabilizes over time (Bravo et al., 2005, 2007, Kim et al., 2008, Park et al., 2010, Lee et al., 2014). Fig. 1 shows a common EGR cooler effectiveness reduction feature with and without an EGR catalyst. In more severe cases the cooler is clogged and failed (Lance et al., 2014). Accordingly, these matters should be resolved in automotive industry.

A large number of researchers have studied stabilization characteristics in many ways. One of the plausible theories is a removal mechanism. And so, this article reviews the fouling deposition and the removal mechanisms as well as its morphology and properties. On the basis of these, a conceptual deposit and removal model is suggested to help further research.

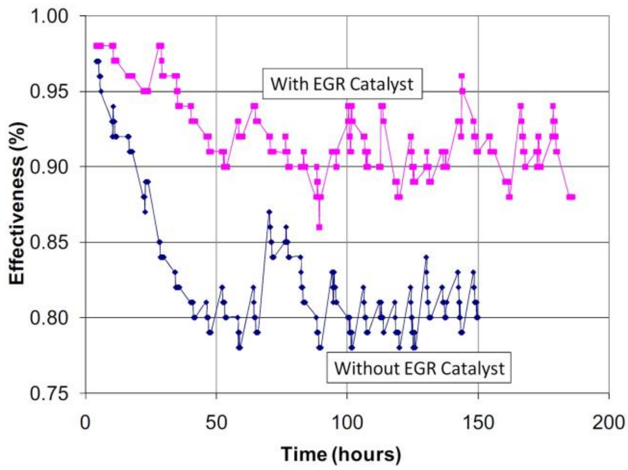

Fig. 1. Diesel EGR cooler effectiveness versus engine running time, without and with an EGR catalyst (Hoard et al., 2007).

DEPOSITION

Hoard et al. (2008) comprehensively researched the composition and characteristics of EGR cooler deposition. They showed that most of deposit is comprised of particulate matter (mostly soot) and condensation of hydrocarbons, water and acids. Accordingly, the basic theories of particulate matter (PM) deposition and condensation are briefly summarized in this section. Also, the presence of large particles is reviewed as well.

1. Particulate Matter Deposition - Thermophoresis

It is known that the majority of diesel soot particles have diameter between 10 nm and 300 nm, and their mean value is around 57 nm (Harris et al., 2002 and Choi et al., 2014). Fig. 2 is a fractional distribution graph of typical diesel soot diameter. Based on this actual exhaust particle size data, Abarham et al. (2010a) carried out modeling work to identify the most dominant deposit mechanism among the five possible factors.

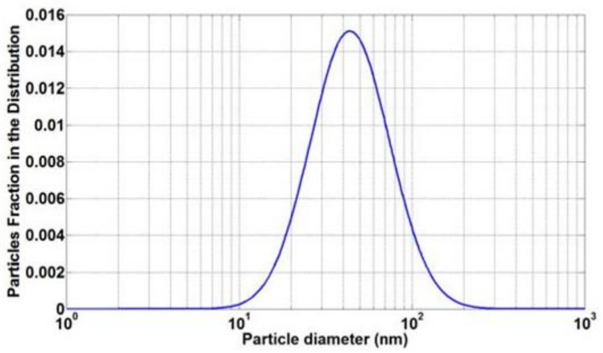

Fig. 2. Diesel EGR soot particles diameter fractional distribution, mostly in 10 nm ~ 300 nm (Harris et al., 2002, modified by Abarham et al.).

They conducted simulations and compared each of deposition velocities in thermophoresis, eddy diffusion, turbulent impaction, electrostatics, and gravitational drift using physical equations. They concluded that the thermophoretic deposit velocity is the dominant mechanism in submicron size particles, as shown in Fig. 3. Thermophoretic velocity is more than 100 times higher than all of the other factors.

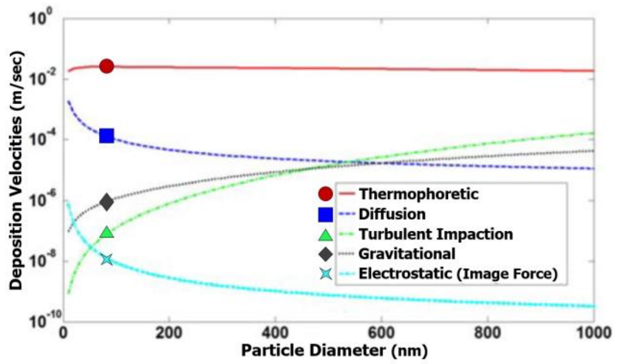

Fig. 3. Comparison of various deposition mechanisms for submicron particles at 600K (Abarham et al., 2010a).

Thermophoresis is a particle motion created by temperature gradient. When a temperature gradient is present, particles travel to the colder side. This force is caused by a phenomenon that the hotter molecules have higher velocity because of their larger kinetic energy. Consequently, a net force is created toward the colder area, and in the EGR cooler case, particles are carried from the gas flow to the boundary layer near the surface. After this transport, particles stick to the wall side mostly due to the Vander Waals forces (Hamaker, H.C., 1937).

Eq. (1) expresses the thermophoretic velocity toward cold surface (Talbot et al. 1980). ∇T is temperature gradient, so it demonstrates that the thermophoretic velocity is linearly affected by temperature gradient between coolant and deposit surface.

$$V_{th} = -K_{th}\frac{\nu}{T}\nabla T \qquad (1)$$

(K_{th}: thermophoretic coefficient, ν: gas kinematic viscosity)

2. Condensation

Condensation is another major cause of EGR cooler fouling. The types of condensation are typically classified into three categories; organic (hydrocarbon), water vapor, and acids condensation. Condensation occurs when the surface temperature of the cooler is below than the dew point of each species at its own partial pressure. This means heavy and high concentration species are condensed more (Warey et al., 2012). Figure 4 shows a form of condensate film when a free stream of a gas is in a certain pressure P and temperature T with some different species and cold surface.

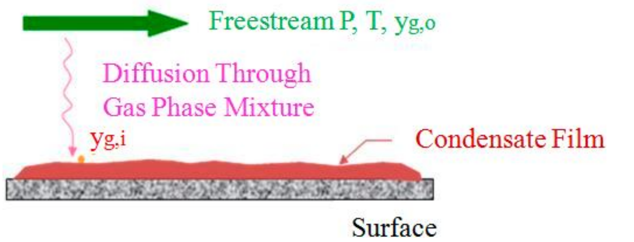

Fig. 4. Condensation film forms on a surface from Hoard et al. (2008).

Abarham et al. (2009a) describes the phenomenon of interface mass transfer to the point of kinetic theory as a difference between two quantities; a rate of molecular arrival from the vapor phase to the interface and a rate of molecules departure from the liquid surface towards the gas phase. Accordingly, when condensation occurs, the arrival rate is higher than departure rate. In terms of condensation rate, mass condensation flux from the gas stream to the cold surface is defined by Eq. (2). As seen in the equation, the mass flux is a function of the mole fraction of species in gas flow and that of at the interface. (Collier and Thome, 1996)

$$j_{g,i} = [0.021\times \mathrm{Re}^{0.8}\frac{\mathrm{Pr}^{1/3}}{Sc^{2/3}}\frac{\alpha}{D}]\,\rho_g \ln\left(\frac{1-y_{g,i}}{1-y_{g,o}}\right) \qquad (2)$$

$$y_{g,i} = \frac{P_{g,i}}{P_{total}},\; y_{g,o} = \frac{P_{g,o}}{P_{total}}. \qquad (3)$$

In the Eq. (2), the values in square bracket become a dimensionless mass transfer coefficient, ρ_g is gas density, and $y_{g,i}$ and $y_{g,o}$ is inner (interface) and outer (bulk mixture) gas mole fraction respectively. Also each mole fraction can be calculated by the ratio of their partial and total pressure like Eq. (3).

3. Large Particles

In addition to these two deposit factors, one point that cannot be ignored is large particles in EGR cooler. Most literature discusses and analyzes only small size particulate matter which is less than 1000 nm (1μm). A possible reason is that particle size analyzers are typically quantifying only smaller particles (smaller than 1 μm) due to their inertial separator usage. Hoard et al. (2012) observed large particles in diesel engine exhaust using their own test stand and MATLAB software.

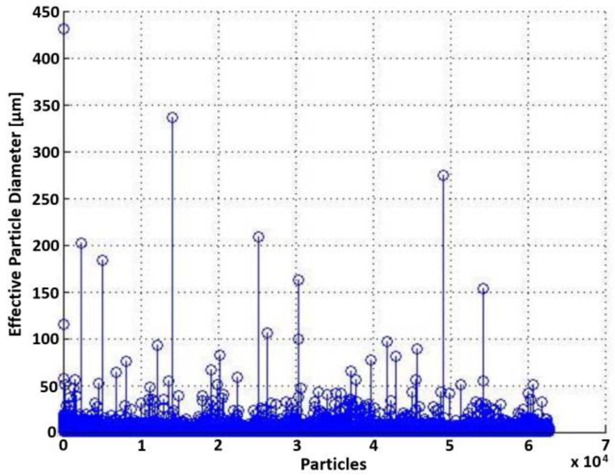

Fig. 5. Particle size for each of 60,000 measured particles at engine out from Hoard et al. (2012)

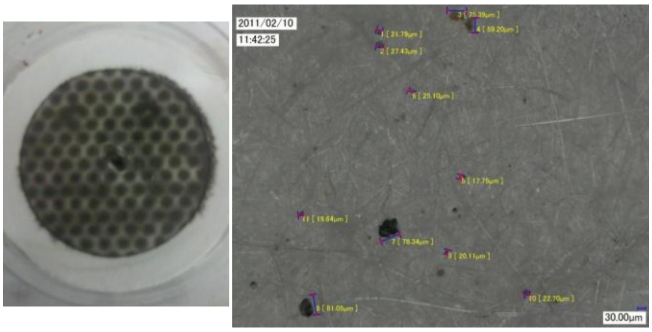

Fig. 6. Typical filter after 2 minutes exposure (left) and image of large particles on fiber glass filter (right), 200x magnification, image area 1.72 mm by 1.29 mm. (Hoard et al., 2012).

They measured particle size and numbers in three different locations with fiberglass filters and a digital microscope. The left hand side of Fig. 6 is the filter darkened by exhaust soot for two minutes. Then, they took a microscope image and counted particle diameter and numbers using software. For the engine exhaust side, maximum 450 μm and mostly tens of μm particles are detected, and total more than 60,000 particles >1μm are measured (Fig. 5). Also, in the particle number case, around ~10^3 large particles were in 20 liter of exhaust, compared to ~10^7 per 1 cubic centimeter of nanoparticles. These large particles should be affected by gravity and turbulent impaction effects in the cooler, unlike the nanoparticles.

MORPHOLOGY AND PROPERTIES

EGR cooler deposit morphology and properties are widely thought of as important factors of effectiveness stabilization and removal mechanism. So, recent studies of deposition morphology and properties are described below.

1. Morphology of Deposition

Surface Current optical observation research shows that the EGR cooler deposit surface is not flat. The flatness of the top layer is important because convective heat transfer inside of the tube is proportional to the heat exchanging surface area. Accordingly, Salvi et al. (2014) calculated the surface area ratio of 24 hours deposit using microscope and MATLAB codes, and their deposit area was as much as 120% larger than for a flat surface at 379 μm deposit thickness.

Li et al. (2014) also measured deposit layer evolution with surface area ratio change during 37 hours. The rate of depth increase tends to start stabilization after 22.5 hours deposition. In addition, their observation shows that the area ratio of deposit reaches a peak and then gradually decreases back toward 100% ratio. Figure 7 shows their surface layer evolution between 22.5 and 31.5 hours deposition. It is obvious that the bumps in the left hand side picture were disappearing by 9 hours deposition.

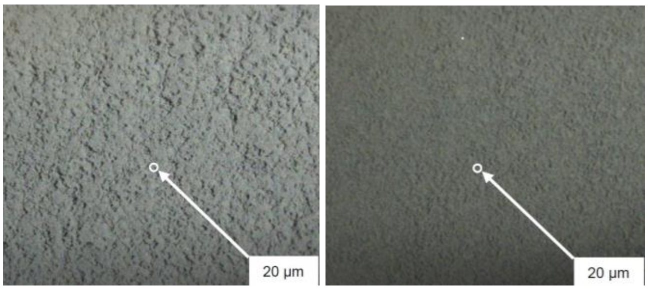

Fig. 7. The comparison of deposit layer surface morphology at 22.5 hour (left) vs. 31.5 hour (right) of deposition (Li et al., 2014)

Also, they pointed out that individual particles on the surface layer grew in size and combined to each other forming dune like particle groups in the size of 20 μm or above which can move on the surface or be blown away from the surface by the gas flow.

Porosity EGR cooler deposit is known to be high porous. Lance et al. (2009) directly measured porosity of deposit layer with three different fuels, ultra-low sulfur diesel, and 5% and 20% volume blend of soy biodiesel in ULSD. Firstly, they measured each of deposit density and got the mean value to 0.035 g/cm^3. Then the calculated porosity was found to 0.98 using the soot particle density 1.77 g/cm^3. (Park et al. 2004)

Figure 8 simply illustrates the deposit porosity. In case of high rate of hydrocarbon in exhaust gas, more soluble organic fraction is able to be condensed in porous space. Because the thermal conductivity of layer can be affected by SOF contents, condensed hydrocarbon study is quite important.

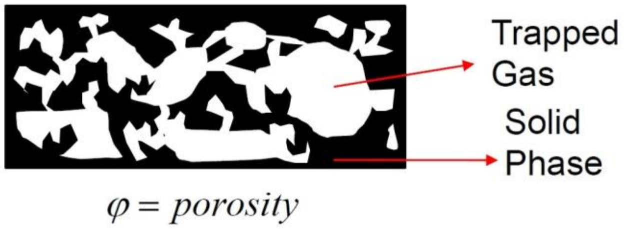

Fig. 8. Schematic of porous deposit layer (Styles et al., 2010).

Soluble Organic Fraction content Sluder et al. (2008) conducted experiments varying with gas flow rate, coolant temperature, and oxidation catalyst to identify SOF contents. The result showed that lower temperature of coolant increased condensed hydrocarbon mass, and an oxidation catalyst reduces deposition of hydrocarbons. Plus, the GC/MS result of deposition indicated that C_{15} to C_{32} hydrocarbons were condensed in cooler. This range corresponds with very heavy end of ULSD, and with lubricant oil. Also, they showed an average mass ratio of hydrocarbon to soot in the deposit; it was lower than 10 percent.

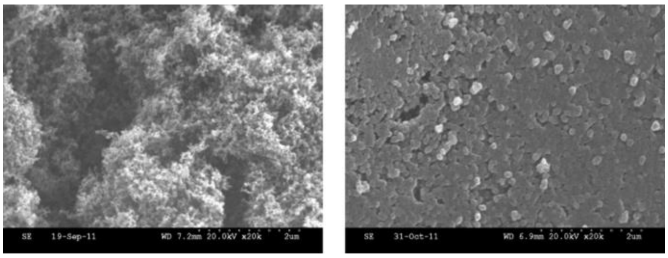

Fig. 9. Effect of coolant temperature on deposit micro-structure, 85ºC (left), 40ºC (right) coolant. (Prabhakar and Boehman, 2013).

Also, Prabhakar and Boehman (2013) led further research of effect of engine operating condition and coolant temperature. They also gained more deposit mass in the lower coolant case, and the deposit microstructure was entirely different under 85 ºC and 40 ºC coolant condition. As Fig. 9 shows, higher coolant condition deposits were coarse and most of deposit was soot (dry soot condition). But lower coolant condition deposit was bigger and more hydrocarbon contents (wet soot condition). Also, micron size big particles were observed on the surface. It is presumed that the differences are due to the high hydrocarbon condensation in the low temperature case.

Also, their pyrolysis-GC chromatographs indicated that the cold coolant condition (40ºC) had more Aliphatic (heavy hydrocarbon) and somewhat less Aromatic hydrocarbons than higher coolant condition (85ºC).

2. Properties of Deposition

Thermal properties of the layer are able to be a good basis to understand removal mechanism. In this paragraph, measured thermal conductivity and deposit density is reviewed.

Thermal Conductivity Salvi et al. (2014) directly measured thermal conductivity of deposit layer with varying hydrocarbon ratio. They also included a bake out experiment. Firstly they built a 379 µm of deposit layer during 24 hours, and then measured heat flux and surface temperature of the deposit. The average of calculated value with area ratio was approximately 0.047 W/mK, prebake case in left graph of Fig. 10. Then they baked the deposit layer to remove volatile fraction with 120 ºC heated air (bake 1 case) and 150 ºC air (bake 2 case) for 1 hour. After bake out, the deposit conductivity slightly decreased compared to the pre-bake case, and the behavior with surface temperature continually decreased with increasing temperature. This seems principally due to higher porosity by volatilized low end hydrocarbon species as their TGA result shows in right hand side of Fig. 10. But, they observed other noticeable phenomena in the surface: one is deposit thickness reduction, and another is the reduction of area ratio from 120% to 112%. Accordingly, the slight reduction of conductivity was a comprehensive effect of all these factors.

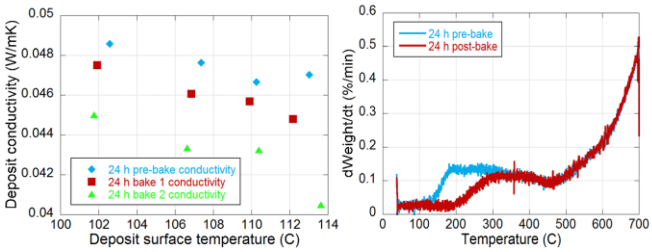

Fig. 10. Deposit conductivity for pre-bake, bake1 and bake2 (left), TGA on pre- and post- bake deposit layer (right) (Salvi et al., 2014).

Lance et al. (2009) also calculated thermal conductivity of deposit layer using surrogate tubes with measured density, diffusivity, and specific heat capacity. Their calculated conductivity was 0.041 W/mK and this value is little lower than the result of Salvi et al. However, considering that it was ex-situ experiment and volatile species were outgassed in their first heating step, their two values are essentially equal.

Density The density of deposit layer is usually thought to be related to porosity. Lance et al. measured the density of deposit, and the value was 0.0316, 0.0363, and 0.0379 g/cm^3 for ULSD, B5, and B20 fuels respectively. This is only 2 percent of normal soot, so it is quite reasonable that the thermal conductivity of the layer is only 1.5 times higher than air (0.025 W/mK). Also, Styles et al. (2010) measured the density of high and low hydrocarbon condition. The high HC case was 0.050~0.064 g/cm^3 and lower HC case was 0.032~0.043 g/cm^3.

REMOVAL MECHANISMS

Currently, significant research is ongoing to identify the reason for effectiveness stabilization on EGR coolers. In the literature, two stabilization factors are generally mentioned:

- The build of an insulating layer causes the surface temperature to gradually increase. As the flow area reduces, the gas velocity increases. However, if this is the only reason for stabilization, then the surface temperature must reach gas temperature (or else thermophoresis will cause continued deposition). This can only happen if effectiveness drops to zero. Various models have shown that this does not happen in EGR coolers. Instead, either some other mechanism causes stabilization or else the cooler plugs.

- Some mechanism causes deposit material to be removed. This may be blow out, spalling, etc. These mechanisms are discussed below.

1. Water Vapor Condensation

When the mole fraction of water vapor in inlet gas is greater than it on the surface layer, water vapor is condensed on the cooler surface. Abarham et al. (2012) conducted experiments with two hypotheses to verify the effect of EGR cooler cool down and reheat. One possibility was that deposits would crack and flake due to thermal expansion difference between the metal and the deposit layer. To explore that, a deposit layer was built, and then the flow changed from exhaust to air. The coolant temperature was cycled from exhaust temperature to room temperature. Imaging showed no effect on the deposit layer. Thus, differential expansion does not seem to cause deposit removal.

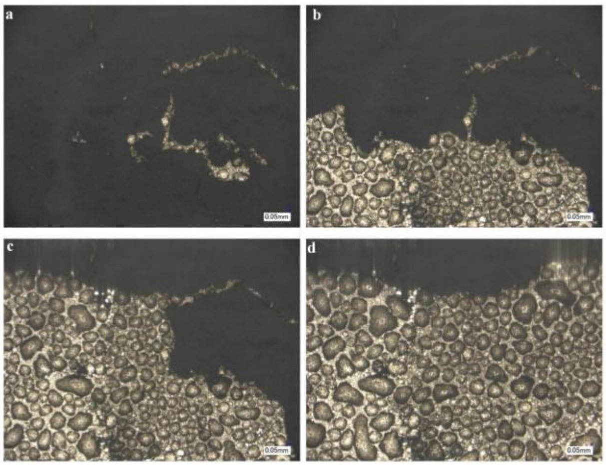

Fig. 11. Deposit flakes when specimen temperature was 20 ºC case, there was 1 min internal between each images 50x magnification (Abarham et al., 2013b).

A second possibility was water condensation. To explore this, the same experiment was run with exhaust (containing about 8% water) instead of air. As the coolant temperature dropped below 40°C (the dew point of water in this exhaust stream), large scale deposit flaking occurred as shown in Fig. 11. As soon as the flakes blew away, water droplets were visible on the metal beneath the deposits. Water, including acids from the exhaust, can permeate the porous deposit layer and release the deposit from the surface due to bond loosing between deposit and cooler surface.

In addition, Warey et al. (2013) conducted experiments on the influence of water vapor while varying the amount of condensed HC on deposit layer. On the dry HC layer with high porosity, the removal rate was high, but there was not noticeable removal in wet HC condition case. This result coincides with the hypothesis that condensed water is hard to permeate through the hydrophobic wet deposit layer.

In another case, Kalghatgi (2002) performed a deposit removal experiment on the piston head in the combustion chamber with varying the factors of water and fuel. Their result said that the water vapor was a significant deposit removal factor. Even though their combustion chamber had different temperature and pressure condition than the EGR cooler, a similar mechanism probably caused loosening the deposit from the metal surface.

While it is established that layers not containing excessive hydrocarbon condensation can be removed by water condensation, practical application of this method has issues. A coolant temperature low enough to provoke condensation is generally only available on engine cold starts. However, EGR flow is typically limited on cold starts due to combustion limits. Further, on cold start the engine control strategy is usually made to rapidly heat the catalysts system to reduce emissions. This process generally includes very high HC levels in the exhaust, intended to generate large exotherm across the upstream oxidation catalyst. Thus, flow of EGR during this catalyst heat mode would introduce large HC in the deposits. To avoid that, EGR cooler operation on cold start is generally not available.

2. Gas Flow Shear Stress

Another important removal factor on deposit layer is shear stress that must arise from gas flow. Sluder et al. (2013) investigated on the effect of shear stress on deposit removal. They approached in two ways, in-situ and ex-situ removal. In their in-situ experiments, a fouling layer was generated during 8 hours on the tubes. At that time, a particle filter was added in the exhaust flow stream for 2 hours. The filter removed incoming soot particles. If there is a steady state removal mechanism, one would expect the cooler effectiveness to begin to recover. However, the thermal resistance result showed the effectiveness stopped increasing and stabilized but did not recover like the graph in Fig. 12. The result suggests that the shear stress is not a major factor of removal mechanism, but it might have been due to other reasons on experiments such as flow rate decrease.

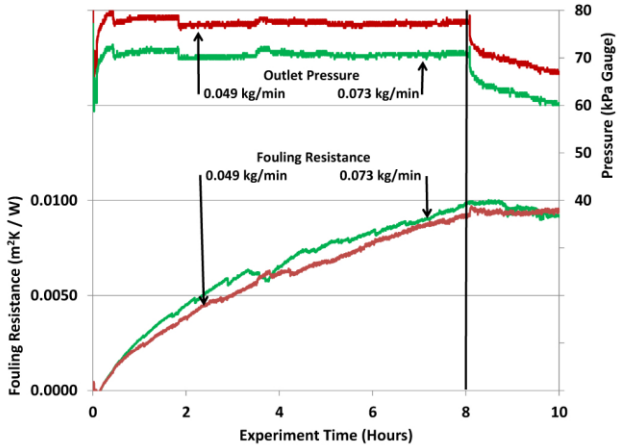

Fig. 12. Fouling resistance and pressure trends from in-situ removal experiment; Red line ≈ 30 m/s and Green line ≈ 43 m/s. (Sluder et al., 2013)

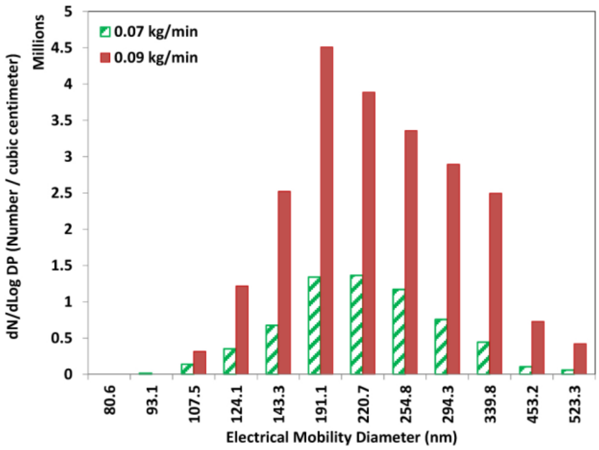

Fig. 13. Particle size results for particles removed at 0.07 and 0.09 kg/min flow rate (Sluder et al., 2013).

The same researchers explained a critical velocity and removed particles in an ex-situ experiment. Firstly, they loaded several deposited surrogate tubes, and the tubes were installed onto a test rig that allowed blow out with ambient air through the tube. Then the removal rate and particle size of the particles were measured with varying air velocity. The result from these experiments showed around 42 m/s of critical velocity and approximately 0.03kPa of shear stress are needed for removal. The velocity of exhaust gas in EGR coolers typically varies between 10 to 30 m/s; from this, one might conclude that particles should not blow out under normal operation. Fig. 13 indicates that the number of removed particles and size result using TSI EEPS. The noticeable part in this graph is that the blown out particle size is larger than normal diesel exhaust one. As discussed above, normal diesel particle size is from 10 nm to 300 nm and the mean value is around 57 nm, but the removed particle size of peak number is around 200 nm. This suggests that the removed particles from the deposit are not simply re-entrained diesel exhaust particulate but rather pieces of the deposit layer.

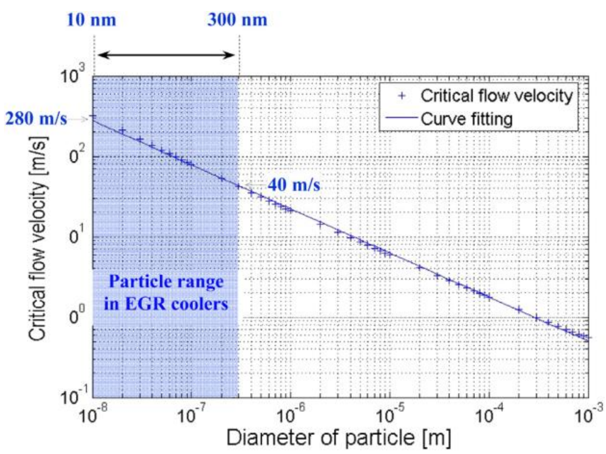

Fig. 14. Critical flow velocity versus particle diameter (Abd-Elhady and Malayeri, 2013).

Abd-Elhady and Malayeri (2013) also studied the particle removal phenomenon and inquired into the relationship between removable particle size and critical gas velocity using a soot generator with ethylene (C_2H_4) (Fig. 14). In their analysis, between 40 m/s and 280 m/s or higher velocity is needed to remove particles in the cooler due to an assumption of diesel particle size; 10 to 300 nm diameter.

From these articles, typical EGR cooler flow rate is lower than their measured critical velocity, but further studies are still remained to verify the shear stress with various combined conditions (Abd-Elhady et al., 2004).

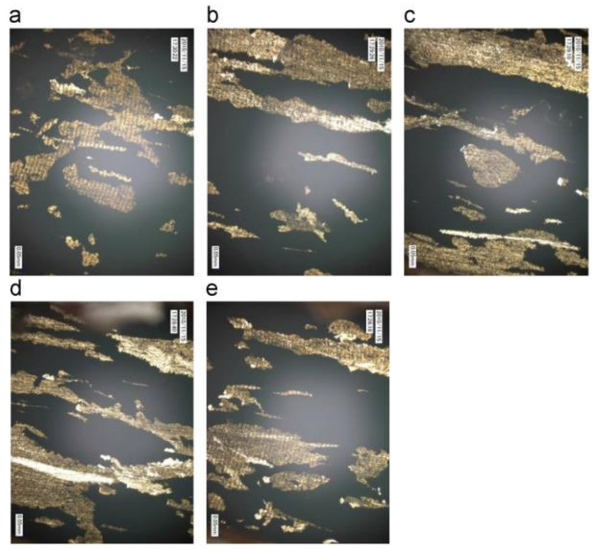

Fig. 15. Series of images along the channel length (flow: left to right) showing the deposit removal due to large flow transient, 50x magnification. (Abarham et al., 2013b).

A somewhat different test of deposit flaking by gas shear flow was run by Abarham et al. (2013b). A series of tests ran in a visualization test rig. By arranging sharp increases of flow rate, well above normal deposition velocity, they observed deposit layer flaking and blowing out as shown in Fig. 15. This result seems to be related both to high velocity and to the sharp increase of flow rate; this is related to the time necessary for the boundary layer to develop.

3. Mud Cracking

Lance et al. (2013) performed a microstructural analysis on a set of aged EGR coolers. The use of these coolers involved varying conditions including flowrate, gas and coolant temperature, HC concentration, and PM level.

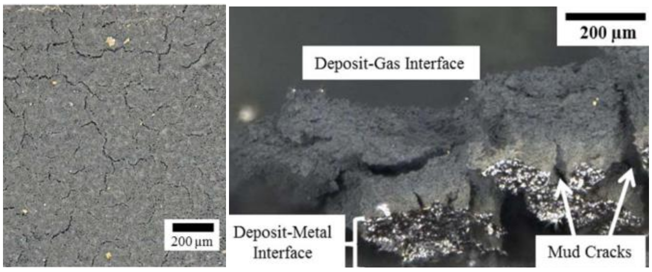

Fig. 16. Mud cracking images. High temperature and low flow rate case (left), high condensed HC case (right). (Lance et al., 2013)

The deposit morphology varied from: dry and flaky, sometimes with mud cracks; hard varnish; or oily wet soot. Among the samples, they observed mud cracking in two cases. One was high inlet gas temperature case (left hand side of Fig. 16) which may be caused by the loss of HC in the deposit, and the other was high hydrocarbon case due to deposit densification (Fig. 16, right).

4. Bake out

As mentioned in the thermal conductivity section, Salvi et al. (2014) observed that the thickness and area ratio are decreased with an hour 120ºC (346µm, Area Ratio 112%) and 150ºC (320µm, AR 112%) bake out experiments. Figure 17 shows the microscope images before and after bake out experiments. The prebake surface seemed fragile, with dendritic features while the post bake one had more clumps of deposit.

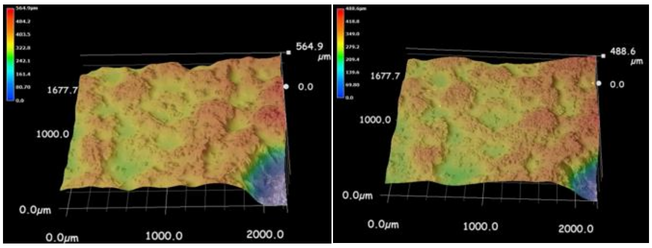

Fig. 17. 3D image of deposit surface after 24h deposit build (left), after bake out case (right), 150x magnification. (Salvi et al., 2014).

Also, in the first bake out test, they noticed a mild shear removal in a quite low flow velocity which is less than 8 kg/h (= 10.1 m/s). Several researchers maintained that quite a high velocity is needed for blowing out, but this showed a possibility of shear removal in a low velocity condition with bake out. And in the following bake out test (150ºC), although a particle movement was not observed, an additional thickness reduction was shown with constant area ratio. This compaction was possibly because a higher kinetic energy of the layer enabled the settling down of deposit layer into a lower porosity structure.

CONCEPTUAL MODEL

The above is a brief compendium of research done on EGR cooler deposits. Given these research results, we can begin to form a conceptual model of the fouling phenomena in diesel exhaust. Mathematical models have been developed for many of the phenomena but not yet for all.

1. Deposition

The primary factor in deposit deposition is the thermophoretic deposition of soot particles from the exhaust gas. This is inevitable: any cold surface in contact with hot gas will create the thermal gradient that drives particles to the surface. The equations for this are presented in a number of papers and summarized above.

The soot deposition due to thermophoresis depends on the temperature gradient. As the layer grows deeper, the top surface of the layer grows hotter and thus thermophoresis decreases. Higher gas flow velocity at constant soot concentration increases the soot deposition rate, but decreases soot capture efficiency. As the deposit layer grows, the cross section area of the tubes decreases so that a constant engine EGR rate requires a higher velocity in the EGR tubes. This also tends to reduce the rate of deposit growth.

A second important deposition is condensation. When the surface temperature is lower than the dew point of any component in the gas, condensation will occur. This is relevant to water, hydrocarbons, and acids in diesel exhaust. The equations for condensation are well established and have been published by Abarham et al. (2009a) and summarized above. For water, the dew point is typically around 40°C but varies with the water content, which in turn varies with engine air-fuel ratio.

Hydrocarbons exist in the engine exhaust, from fuel – usually partially oxidized – and lube oil. Only the heavier hydrocarbons in fuel, or the lube oil hydrocarbons, are heavy enough to have dew points in the range relevant to EGR cooler fouling. Typically C_{18} to C_{30} HCs are found in the deposits. Normal diesel engine calibrations generally have very low HC content, so the HC is only a small part of the deposit mass, < 10% (Teng et al., 2009). However, under some conditions some engines have higher HC levels resulting in heavy wet soot. Such soot does not seem to be subject to the removal mechanisms, and tends to cause cooler plugging eventually (Sluder et al., 2014).

Acids form in exhaust condensate. Sulfuric, nitric, acetic, and formic acids are present in low concentrations. Exhaust condensate typically has pH around 2. The actual levels will of course vary with fuel sulfur level, engine out NOx concentration and so on. McKinley (1997) has modeled sulfuric acid condensation, which occurs below about 105°C. Acids form a very small percentage of the deposit mass.

2. Deposit morphology

As particles reach the surface, they stick. Initially, very small particles stick to the wall primarily due to Vander Walls force (Abarham et al., 2010b). As more particles build, the transformation from a large number of very small, non-spherical soot particles into a weak porous solid is not well modeled. The soot particles tend to be very small primary particles agglomerated into fractal agglomerates. These stick together and intertwine. The soot particles have many sites that are active for adsorption of hydrocarbons. For relatively dry soot, the HC is probably not present as a liquid on the surface of the particles, but rather as adsorbed species.

As the deposit ages, it is possible that the HCs tends to cross link and polymerize. It is known that such reactions happen in lube oil HCs in the presence of NO_2; this is a major mechanism of lacquer formation in engine crankcases. Such reactions may tend to cause the deposit layer to become more rigid as it ages.

Some simplified deposit models have assumed that the deposit layer is flat. However, in-situ observations clearly show non-flat layers including dune-like shapes (Li et al., 2014). This probably should not be surprising since we know that, for instance, desert sand does not form a flat layer but rather tends to form dunes. Figure 18 shows sketches and real satellite images of sand dunes. (a), (b), (e), and (f) indicate one direction flow cases similar to EGR cooler.

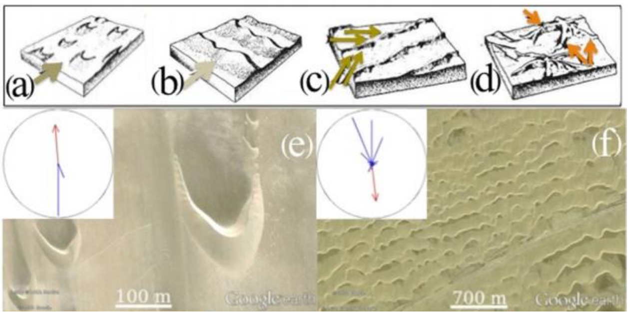

Fig. 18. The four main types of dunes occurring in nature. In the box on top: barchans-(a), transverse dunes-(b), longitudinal dunes-(c), and star dunes-(d). Arrows indicate the prevailing wind directions (Greeley and Iversen 1985). In the bottom box: satellite images of barchans in Peru-(e) and transverse dunes in Bahrein-(f). (Kok et al. 2012).

Also, Abarham, in an unpublished study, made a simple model assuming that soot is spherical and approached a surface due to thermophoresis and gas flow, at a small angle. If a particle hits the surface it sticks. If another particle comes along that would otherwise stick just downstream, it will instead hit this first particle and stick to it. Together, they shield a larger area. The Monte Carlo model, as simple as it was, predicted a surface with wavy structure rather than a flat one. So, perhaps simple models can describe the surface texture. Figure 19 is a schematic of sand bump and wind profile in nature. Maximum erosion would always occur upstream of the crest, and sand would be deposited on the bump, thus leading to dune growth. (τ_{max} and q_{max} indicate the positions of maximum shear stress and sand flux, and L_{sat} is saturation length) This ongoing process keeps the sand surface wavy.

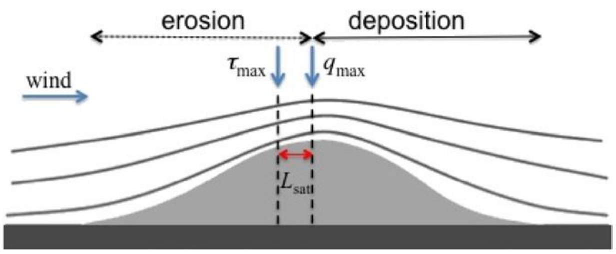

Fig. 19. Schematic diagram showing streamlines of the wind flow over a bump. The bump grows if the maximum flux is reached upwind of the bump crest. (Fourriere et al., 2010, modified by Kok et al.).

Experiments show that if the deposit layer gets wetted by HC, mud cracks form. Visualization rig has observed that this occurs during the wetting process, presumably because surface tension of the liquid pulls the soot into a smaller volume (Salvi et al., 2014). The conditions under which this may happen in actual vehicle use are not clear.

The bake-out experiments of Salvi et al. (2014) indicate that aging conditions can affect the layer properties. In those experiments, baking the layer at temperatures of 100~150°C under low air flow (too low to blow soot out of the layer) caused significant shrinkage in the layer depth. Surprisingly, the thermal conductivity was essentially unchanged while the layer depth reduced by 30%. As a result, such a bake out improved EGR cooler effectiveness.

3. Removal

Abarham et al. (2009b, 2011) and others have modeled the deposition mechanisms. These models fit very well a set of data developed by Sluder et al. and Styles et al. (2011). The experiment exposed simulated EGR tubes to exhaust for three hours and varied flow rate, coolant temperature, exhaust temperature, soot concentration, and HC concentration as independent, orthogonal variables.

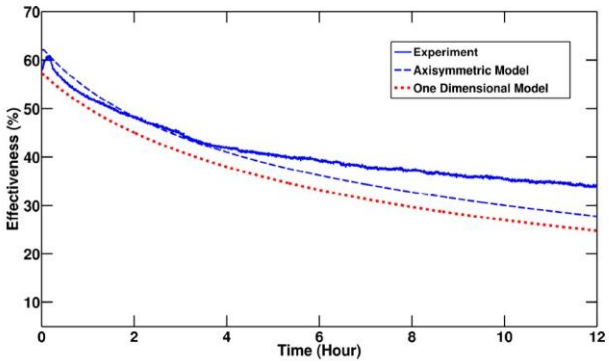

Fig. 20. The effectiveness comparison between experiment and models for a longer time (Abarham et al., 2011).

However, although the models fit the three hour data very well, they did less well for longer times as seen in Fig. 20. Abarham et al. (2011) concluded that the models must include a removal mechanism. The exact mechanism of this removal remains to be completely modeled. One can assume a simple equation form, such that some of the deposit "blows away", perhaps an amount proportional to the total deposit mass. Such assumptions lead to equations that match data quite well. However, if we assume this removal is gas flow shear removing particles, then it conflicts the Sluder's (2013) in-situ and ex-situ experimental results. Further research is needed to resolve this apparent conflict.

It is clearer that conditions leading to water condensation can remove deposits. As mentioned above, there are emission control strategy reasons why this may not be possible in real engines.

4. Conceptual Model

With these deposit and removal ideas, a conceptual model is built up. Fig. 21 illustrates a conceptual deposit thickness versus engine operation time. Pre- and post-stabilization range is separated by stabilization time, which is typically 50 to 100 hours. Clogging occurs if a removal mechanism is not able to keep growth low enough; eventually the layer fills the space and the cooler clogs.

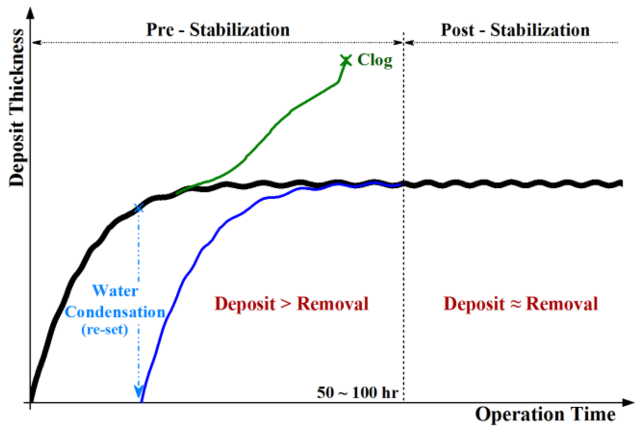

Fig. 21. A conceptual graph of deposit thickness versus engine operation time.

In the pre-stabilization range, both deposit and removal occur but deposition dominates the removal. If water condensation occurs among several removal mechanisms, the deposit may be washed out entirely. So, deposition will restart as illustrated in Fig. 21. After stabilization, even though there is a fluctuation, the mean values of deposit thickness, density, and the amount of heat transfer are consistent. The fluctuation is caused by repetitive change of the removal and deposit rate, which cannot be exactly equal, but the total will be near constant.

Figure 22 introduces conceptual models of deposit and removal mechanism. On the upper side of illustration, the deposit mechanism model is shown and it is a standard soot and HC deposition. The main point in this model is the deposition of HC and the shape of the top surface. Initially HC deposits on the top surface and may come down to the cold surface as the operation time goes by. As a result, it is possible that the HC fraction on the lower surface becomes higher. Also, the top surface remains wavy, not flat due to the continuous removal even after stabilization.

The removal mechanism is illustrated on the lower part of Fig. 22. The previously described removal mechanisms are categorized into 5 types; water condensation, large particle, shear flow removal, mud cracking, and bake out. Since the water condensation washing out mostly happens in pre-stabilization, it is not described in Fig. 22 but in Fig. 21.

Firstly, the large particle removal (A) is introduced in the post-stabilization section. When a micron size large particle enters the EGR cooler, it may land on the fouling layer and makes a dune style surface. The top side of the dune suffers erosion due to the maximum shear stress and overall HC loss with hot inlet gas. Also, in the outlet side, normal exhaust soot particles deposit and stick on the surface. After a certain amount of time with this effect, the dune gradually moves to outlet side.

Also, removal caused by shear flow and mud cracking is illustrated in (B). Shear flow removal and mud cracking are different removal factors, but the restoration tendency is quite same, so these two are described together. If mud cracking occurs on the surface, small valleys are created. And, when the deposit goes through an instant shear stress over a critical velocity, the shear removal occurs. In this case, many small particles or a large lump removal may occur. So, this model shows lump particle removal and cracks on the deposit. After cavities form due to shear stress or cracking, new exhaust soot particles stick in it, and the hole tends to return to its previous surface shape.

The third one is bake out case (C). As hot gas flows, HCs in the deposit slowly evaporate and soot particles shrink. In this step, some small particles may leave the surface, and additional soot particles with HC are attached again with enhanced temperature gradient. As Salvi (2014) showed, even though thickness is decreased, the thermal conductivity remains same. So the temperature gradient should be increased as operation goes by and additional deposition occurs. Then the surface is restored to previous condition.

In the EGR cooler fouling, all of these removal and deposit mechanism are comprehensively applied together. Therefore, the effectiveness is able to be consistently maintained with these equalized mechanisms.

SUMMARY

As a result of research by a number of groups over a significant time period, many aspects of diesel engine EGR cooler fouling are well understood though a few remain to be fully defined.

1. Deposit mass is dominated by thermophoretic deposition of soot.
2. Under some conditions water and/or acid condensation can affect the deposit properties.
3. Deposit layers have complex surface profiles with area changes sufficient to affect heat transfer.
4. “Heavy wet soot” should be avoided by maintaining low engine-out HC
5. Deposit mud cracking is associated with high HC concentration.
6. Sufficiently high gas flow blows particles off the deposit surface, but experiments suggest this may not happen at normal flow conditions.
7. A removal mechanism must be present in order to explain the tendency for cooler effectiveness to stabilize. However, the exact mechanism remains to be clearly defined.

NOMENCLATURE

AR	Area Ratio
EEPS	Engine Exhaust Particle Sizer
EGR	Exhaust Gas Recirculation
HC	Hydrocarbon
PM	Particulate Matter
SOF	Soluble Organic Fraction
TGA	Thermal Gravimetric Analysis
ULSD	Ultra Low Sulfur Diesel

Fig. 23. A conceptual model of deposition and removal mechanism.

D Tube Inner Diameter
K_{th} Thermophoretic coefficient
Pr Mean flow Prandlt Number
Re Reynolds Number
Sc Schmidt Number
T Absolute Temperature [K]
V_{th} Thermophoretic velocity [m/s]
$y_{g,i}$ Mole fraction of vapor at interface
$y_{g,o}$ Mole fraction of vapor in bulk mixture
α Thermal Diffusivity [m^2/s]
ν Gas kinematic viscosity [m^2/s]

Subscript
g gas
i inner
o outer

REFERENCES

Abarham, M., Hoard, J., Assanis, D., Styles, D., Curtis, E. W., Ramesh, N., Sluder, C.S., and Storey, J. M., 2009a, Modeling of thermophoretic soot deposition and hydrocarbon condensation in EGR cooler, *SAE Int. J. Fuels Lubr.* 2(1): 921-931

Abarham, M., Hoard, J., Assanis, D.N., Styles, D., Curtis, E.W., Ramesh, N., Sluder, C.S. and Storey, J.M., 2009b, Numerical modeling and experimental investigations of EGR cooler fouling in a diesel engine, *SAE Technical Paper*, No. 2009-01-1506.

Abarham, M., Hoard, J., Assanis, D., Styles, D., Curtis, E., Ramesh, N., 2010a, Review of soot deposition and removal mechanisms in EGR coolers, *SAE Int. J. Fuels Lubr.* 3(1):690-704.

Abarham, M., Hoard, J.W., Assanis, D., Styles, D., Sluder, C.S., and Storey, J.M., 2010b, An analytical study of thermophoretic particulate deposition in turbulent pipe flows, *Aerosol Science and Technology,* 44(9), 785-795.

Abarham, M., Zamankhan, P., Hoard, J., Assanis, D., Styles, D., Sluder, S., and Storey, J., 2011, Eulerian CFD Models to Predict Thermophoretic Deposition of Soot Particles in EGR Coolers, *17th Directions in Engine-Efficiency and Emissions Research Conference (DEER),* Detroit, MI, October.

Abarham, M., Chafekar, T., Hoard, J., Styles, D., and Assanis, D., 2012, A visualization test setup for investigation of water-deposit interaction in a surrogate rectangular cooler exposed to diesel exhaust flow, *SAE Technical Paper,* No. 2012-01-0364.

Abarham, M., Zamankhan, P., Hoard, J. W., Styles, D., Sluder, C.S., Storey, J. M., Lance, M.J., and Assanis, D., 2013a, CFD analysis of particle transport in axi-symmetric tube flows under the influence of thermophoretic force. *International Journal of Heat and Mass Transfer,* 61, 94-105.

Abarham, M., Chafekar, T., Hoard, J.W., Salvi, A., Styles, D.J., Sluder, C.S., and Assanis, D., 2013b, In-situ visualization of exhaust soot particle deposition and removal in channel flows, *Chemical Engineering Science,* 87, 359-370.

Abd-Elhady, M.S., Rindt, C.C.M., Wijers, J.G., Van Steenhoven, A.A., Bramer, E.A., and Van der Meer, T.H., 2004, Minimum gas speed in heat exchangers to avoid particulate fouling, *International Journal of Heat and Mass Transfer*, 47(17), 3943-3955.

Abd-Elhady, M.S. and Malayeri, M.R., 2013, Asymptotic characteristics of particulate deposit formation in exhaust gas recirculation (EGR) coolers. *Applied Thermal Engineering,* 60(1), 96-104.

Bravo, Y., Lázaro, J., and García-Bernad, J., 2005, Study of Fouling Phenomena on EGR Coolers due to Soot Deposits. Development of a Representative Test Method, *SAE Technical Paper* No. 2005-01-1143.

Bravo, Y., Moreno, F., and Longo, O., 2007, Improved characterization of fouling in cooled EGR systems, *SAE Technical Paper* No. 2007-01-1257.

Choi, S., Myung, C., and Park, S., 2014, Review on characterization of nano-particle emissions and PM morphology from internal combustion engines: Part 2, *International Journal of Automotive Technology* 15, no. 2 (2014): 219-227.

Collier, J.G. and Thome, J.R., 1996, Convective Boiling and Condensation, 3rd Edition.

Fourriere, A., Claudin, P., and Andreotti, B., 2010, Bedforms in a turbulent stream: formation of ripples by primary linear instability and of dunes by nonlinear pattern coarsening, *Journal of Fluid Mechanics,* 649, 287-328.

Greeley, R., and Iversen, J.D., 1987, Wind as a geological process: on Earth, Mars, Venus and Titan, *CUP Archive,* Vol. 4.

Hamaker, H.C., 1937, The London – Vander Waals attraction between spherical particles, *Physica IV* 10:1058-1072.

Harris, S.J. and Maricq, M.M., 2002, The role of fragmentation in defining the signature size distribution of diesel soot, *J. of Aerosol Science,* Vol. 33, pp. 935-942.

Hoard, J. and Moilanen, P., 1997, Exhaust Valve Seat Leakage, *SAE Technical Paper,* No. 971638.

Hoard, J., Giuliano, J., Styles, D., Sluder, S., Storey, J., Lewis, S., Strzelec, A., and Lance, M., 2007, EGR Catalyst for Cooler Fouling Reduction, *2007 DOE Diesel Engine-Efficiency and Emission Reduction Conference,* Detroit, MI, August 2007.

Hoard, J., Abarham, M., Styles, D., Giuliano, J.M., Sluder, C.S., and Storey, J.M., 2008, Diesel EGR cooler fouling, *SAE Int. J. Engines* 1(1):1234-1250.

Hoard, J., Chafekar, T., Abarham, M., Schwader, R., Upplegger, S., and Styles, D., 2012, Large particles in modern diesel engine exhaust, *ASME 2012 Internal Combustion Engine Division Spring Technical Conference* (pp. 521-530).

Kalghatgi, G.T., 2002, Combustion Deposit Flaking – Studies Using a Road Test Procedure, *SAE Technical Paper,* No. 2002-01-2833.

Kim, H.M., Lee, D.H., Park, S.K., Choi, K.S., and Wang, H.M., 2008, An experimental study on heat exchange effectiveness in the diesel engine EGR coolers, *Journal of Mechanical Science and Technology,* 22(2), 361-366.

Kok, J.F., Parteli, E.J., Michaels, T.I., and Karam, D.B., 2012, The physics of wind-blown sand and dust, *Reports on Progress in Physics*, 75(10), 106901.

Lance, M.J., Sluder, C.S., Wang, H., and Storey, J.M.E., 2009, Direct Measurement of EGR Cooler Deposit Thermal Properties for Improved Understanding of Cooler Fouling, *SAE Technical Paper*, No. 2009-01-1461.

Lance, M.J., Storey, J., Lewis, S., and Sluder, C.S., 2014, Analysis of Lacquer Deposits and Plugging Found in Field-Tested EGR Coolers, *SAE Technical Paper* No. 2014-01-0629.

Lance, M.J., Storey, J., Sluder, C.S., Meyer III, H., Watkins, B., Kaiser, M., and Ayyappan, P., 2013, Microstructural Analysis of Deposits on Heavy-Duty EGR Coolers, *SAE Technical Paper*, No. 2013-01-1288.

Lee, J., and Min, K., 2014, A study of the fouling characteristics of EGR coolers in diesel engines. *Journal of Mechanical Science and Technology*, 28(8), 3395-3401.

Li, H., Hoard, J., Styles, D., Salvi, A., Kini, A., Bieniek, M., Cao, W. and Erickson, N., 2014, Visual Study of In-Situ EGR Cooler Fouling Layer Evolution, *ASME 2014 Internal Combustion Engine Division Fall Technical Conference*, Paper No. ICEF2014-5683.

McKinley, T., 1997, modelling sulphuric acid condensation in diesel engine EGR coolers, *SAE Technical Paper*, No. 970636.

Park, K., Kittelson, D.B., Zachariah, M.R., and McMurry, P.H., 2004, Measurement of inherent material density of nanoparticle agglomerates. *Journal of Nanoparticle Research*, 6(2), 267-272.

Park, S., Choi, K., Kim, H., and Lee, K., Influence of PM fouling on effectiveness of heat exchanges in a diesel engine with fin-type EGR coolers of different sizes, *Heat and mass transfer* 46, no. 11-12 (2010): 1221-1227.

Prabhakar, B. and Boehman, A.L., 2013, Effect of Engine Operating Conditions and Coolant Temperature on the Physical and Chemical Properties of Deposits From an Automotive Exhaust Gas Recirculation Cooler, *Journal of Engineering for Gas Turbines and Power*, 135(2), 022801.

Salvi, A.A., Hoard, J., Jagarlapudi, P.K., Pornphaithoonsakun, T., Collao, K., and Assanis, D.N., Styles, D.J., Abarham, M., Curtis, E.W., 2013, Optical and Infrared In-Situ Measurements of EGR Cooler Fouling, *SAE Technical Paper*, No. 2013-01-1289.

Salvi, A., Hoard, J., Bieniek, M., Abarham, M., Styles, D., Assanis, D., 2014, Effect of Volatiles on Soot Based Deposit Layers, *J ENG GAS TURB POWER*, 136 (11): 11401-11401.

Sluder, C.S., Storey, J.M., Lewis, S.A., Styles, D., Giuliano, J., and Hoard, J.W., 2008, Hydrocarbons and particulate matter in EGR cooler deposits: effects of gas flow rate, coolant temperature, and oxidation catalyst, *SAE Technical Paper*, No. 2008-01-2467.

Sluder, C.S., Storey, J.M., Lance, M.J., Stork, K., and Przesmitzki, S., 2011, Hydrocarbon and Deposit Morphology Effects on EGR Cooler Deposit Stability and Removal, *17th Directions in Engine-Efficiency and Emissions Research Conference (DEER)*, Detroit, MI, October.

Sluder, C.S., Storey, J., Lance, M.J., and Barone, T., 2013, Removal of EGR Cooler Deposit Material by Flow-Induced Shear, *SAE Technical Paper*, No. 2013-01-1292.

Sluder, C.S., Storey, J.M., and Lance, M.J., 2014, Effectiveness Stabilization and Plugging in EGR Cooler Fouling, *SAE Technical Paper* No. 2014-01-0640

Styles, D., Curtis, E., Ramesh, N., Hoard, J., Assanis, D., Abarham, M., Sluder, S., Storey, J., and Lance, M., 2010, Factors Impacting EGR Cooler Fouling: Main Effects and Interactions, *16th Directions in Engine-Efficiency and Emission Research Conference (DEER)*, Detroit, MI, September 27–30.

Styles, D., Curtis, E., Ramesh, N., Hoard, J., Assanis, D., Abarham, M., Sluder, S., Storey, J., and Lance, M., 2011, EGR Cooler Fouling-Visualization of Deposition and Removal Mechanisms, *17th Directions in Engine-Efficiency and Emissions Research Conference (DEER)*, Detroit, MI, October.

Talbot, L., Cheng, R. K., Schefer, R. W., and Willis, D. R., 1980, Thermophoresis of particles in a heated boundary layer, *Journal of Fluid Mechanics*, 101(04), 737-758.

Teng, H., and Regner, G., 2009, Characteristics of Soot Deposits in EGR Coolers, *SAE Technical Paper*, No. 2009-01-2671.

Teng, H., and Regner, G., 2009, Particulate fouling in EGR coolers, *SAE Technical Paper*, No. 2009-01-2877.

Warey, A., Balestrino, S., Szymkowicz, P., and Malayeri, M.R., 2012, A one-dimensional model for particulate deposition and hydrocarbon condensation in exhaust gas recirculation coolers. *Aerosol Science and Technology*, 46(2), 198-213.

Warey, A., Bika, A.S., Long, D., Balestrino, S., and Szymkowicz, P., 2013, Influence of water vapor condensation on exhaust gas recirculation cooler fouling, *International Journal of Heat and Mass Transfer*, 65, 807-816.

Warey, A., Bika, A.S., Vassallo, A., Balestrino, S., and Szymkowicz, P., 2014, Combination of Pre-EGR Cooler Oxidation Catalyst and Water Vapor Condensation to Mitigate Fouling, *SAE International Journal of Engines*, 7(2014-01-0636), 21-31